Dynamics of Colloid Deposition in Porous Media: Blocking Based on Random Sequential Adsorption

ARTICLE *in* LANGMUIR · MARCH 1995

Impact Factor: 4.46 · DOI: 10.1021/la00003a023

2 AUTHORS, INCLUDING:

Menachem Elimelech
Yale University
394 PUBLICATIONS **32,538** CITATIONS

Dynamics of Colloid Deposition in Porous Media: Blocking Based on Random Sequential Adsorption

Philip R. Johnson and Menachem Elimelech*

School of Engineering & Applied Science, University of California, Los Angeles, California 90095-1593

Received November 16, 1994[⊗]

An improved theoretical model is presented for quantifying the dynamics of colloid deposition in granular porous media. The model characterizes the transient aspects of irreversible particle deposition onto spherical collector surfaces where repulsive electrostatic forces between colloidal particles limit deposition to monolayer coverage. The transient deposition rate normally associated with particle deposition is depicted in the model by a dynamic blocking function derived from random sequential adsorption (RSA) mechanics. The RSA blocking function has a nonlinear power law dependence on surface coverage, in contrast to the linear Langmuirian blocking function used in previous dynamic deposition models for porous media. A technique involving the calculation of the jamming limit from experimental particle breakthrough curves is utilized for determining the excluded area parameter, an integral component of the dynamic blocking function. Parameter estimation and curve fitting techniques are not required by the model as all parameter values are calculated *a priori* using available theoretical principles. Parameter values are incorporated into the theoretical model to produce theoretical particle breakthrough curves based on both RSA and Langmuirian dynamic blocking functions. A comparison of theoretical results with experimental particle breakthrough curves demonstrates the utility of RSA mechanics as a means of describing particle blocking dynamics associated with colloid deposition in granular porous media.

1. Introduction

Numerous technological and natural processes are based on the transfer of colloidal particles from liquid suspension onto stationary surfaces. Such processes include papermaking,[1] deep bed filtration,[2] fouling of reverse osmosis membranes,[3] immobilization of biocolloids in soils,[4] transport of colloidal contaminants in groundwater,[5,6] and thrombosis formation on artificial organ surfaces.[7] The broad significance of particle deposition is underscored by the wide array of colloids involved in the deposition process. Recent experimental studies pertaining to particle deposition have dealt with a diverse assortment of particles, including proteins and polypeptides,[8–12] bacteria and viruses,[13–19] various minerals,[20–26] and man-made latex spheres.[27–34]

The development and utilization of theoretical deposition models is one means of attaining a better understanding of colloids and the myriad processes pertaining to colloid deposition. Because particle deposition is an inherently dynamic process that typically exhibits variable kinetics during the course of a depositional sequence, theoretical models designed to address the entire range of deposition from inception to completion must describe the initial kinetics as well as the dynamic aspects of particle deposition.

During the initial stage of deposition, while collector surfaces are essentially devoid of particles, a constant rate of particle deposition is generally observed.[20,30,35] This initially constant deposition rate is often represented by a kinetic rate equation in theoretical models. The kinetics of colloid deposition for bare collector surfaces have been characterized for various types of collector geometries, including the rotating disk,[27,35,36] stagnation point

* Author to whom all correspondence should be addressed.

[⊗] Abstract published in *Advance ACS Abstracts,* February 15, 1995.

(1) Varennes, S.; van de Ven, T. G. M. *Colloids Surf.* **1988**, *33*, 63.
(2) Tien, C. *Granular Filtration of Aerosols and Hydrosols*; Butterworths: Stoneham, MA., 1989.
(3) Hung, C. C.; Tien, C. *Desalination* **1976,** *18,* 173.
(4) Grant, S. B.; List, E. J.; Lidstrom, M. E. *Water Resour. Res.* **1993**, *29*, 2067.
(5) McDowell-Boyer, L. M.; Hunt, J. R.; Sitar, N. *Water Resour. Res.* **1986**, *22*, 1901.
(6) McCarthy, J. F.; Zachara, J. M. *Environ. Sci. Technol.* **1989**, *23*, 496.
(7) Bruck, S. D. *J. Biomed. Mater. Res.* **1972**, *6*, 173.
(8) Feder, J.; Giaever, I. *J. Colloid Interface Sci.* **1980**, *78*, 144.
(9) Feder, J. *J. Theor. Biol.* **1980**, *87*, 237.
(10) Young, B. R.; Pitt, W. G.; Cooper, S. L. *J. Colloid Interface Sci.* **1988**, *124*, 28.
(11) Juriaanse, A. C.; Arends, J.; ten Bosch, J. J. *J. Colloid Interface Sci.* **1980**, *76*, 212.
(12) Aptel, J. D.; Voegel, J. C.; Schmitt, A. *Colloids Surf.* **1988**, *29*, 359.
(13) Gibbons, R. J.; Moreno, E. C.; Etherden, I. *Infect. Immun.* **1983**, *39*, 280.
(14) Moncla, B. J.; Halfpap, L.; Birdsell, D. C. *J. Gen. Microbiol.* **1985**, *131*, 2619.
(15) Cookson, J. T. *Environ. Sci. Technol.* **1970**, *4*, 128.
(16) Scholl, M. A.; Mills, A. L.; Herman, J. S.; Hornberger, G. M. *J. Contam. Hydrol.* **1990**, *6*, 321.
(17) Harvey, R. W.; Garabedian, S. P. *Environ. Sci. Technol.* **1991**, *25*, 178.
(18) Logan, B. E.; Hilbert, T. A.; Arnold, R. G. *Water Res.* **1993**, *27*, 955.
(19) Bales, R. C.; Hinkle, S. R.; Kroeger, T. W.; Stocking, K.; Gerba, C. P. *Environ. Sci. Technol.* **1991**, *25*, 2088.
(20) Marshall, J. K.; Kitchener, J. A. *J. Colloid Interface Sci.* **1966**, *22*, 342.
(21) Bowen, B. D.; Epstein, N. *J. Colloid Interface Sci.* **1979**, *72*, 81.
(22) Rajagopalan, R.; Chu, R. Q. *J. Colloid Interface Sci.* **1982**, *86*, 299.
(23) Kallay, N.; Tomic, M.; Biskup, B.; Kunjasic, I.; Matijevic, E. *Colloids Surf.* **1987**, *28*, 185.
(24) Ryde, N.; Kallay, N.; Matijevic, E. *J. Chem. Soc. Faraday Trans.* **1991**, *87*, 1377.
(25) Rosta, L.; von Gunten, H. R.; Giovanoli, R. *Colloids Surf.* **1991**, *55*, 205.
(26) Puls, R. W.; Powell, R. M. *Environ. Sci. Technol.* **1992**, *26*, 614.
(27) Hull, M.; Kitchener, J. A. *Trans. Faraday Soc.* **1969**, *65*, 3093.
(28) FitzPatrick, J. A; Spielman, L. A. *J. Colloid Interface Sci.* **1973**, *43*, 350.
(29) Gregory, J.; Wishart, A. J. *Colloids Surf.* **1980**, *1*, 313.
(30) Adamczyk, Z.; Zembala, M.; Siwek, B.; Czarnecki, J. *J. Colloid Interface Sci.* **1986**, *110*, 188.
(31) Varennes, S.; van de Ven, T. G. M. *Physicochem. Hydrodyn.* **1987**, *9*, 537.
(32) Sjollema, J.; Busscher, H. J. *J. Colloid Interface Sci.* **1989**, *132*, 382.
(33) Elimelech, M.; O'Melia, C. R. *Langmuir* **1990**, *6*, 1153.
(34) Elimelech, M. *J. Colloid Interface Sci.* **1991**, *146*, 337.
(35) Adamczyk, Z.; Szyk, L.; Warszynski, P. *Colloids Surf. A* **1993**, *75*, 185.
(36) Prieve, D. C.; Lin, M. M. *J. Colloid Interface Sci.* **1980**, *76*, 32.

0743-7463/95/2411-0801$09.00/0

flow,[30,38,39] parallel plate channel,[21,32] isolated sphere,[40-42] and packed beds of spherical collectors[15,19,22-25,28,33,43] and cylindrical fibers.[29]

During the later stages of deposition, variations in the rate of particle deposition arise as particles accumulate on collector surfaces. Accumulation of particles will cause either a rise or decline in the deposition rate, depending on solution chemistry and the surface chemistry of particles and collectors.[2,24,45] In many deposition processes, declining deposition rates arise when excluded area effects of deposited particles hinder subsequent attachment of particles.[22] Excluded area effects are produced when repulsive electrostatic forces emanating from charged particles deposited on collector surfaces create an energy barrier which inhibits subsequent deposition.

When conditions are conducive to the presence of repulsive energy barriers, excluded area effects must be included in the kinetic rate equation in order to account for the dynamic aspects of the deposition process. This is generally accomplished by appending a *dynamic blocking function* to the kinetic rate equation.[46-51] The dynamic blocking function characterizes the probability that deposition will result from a particle–collector interaction by quantifying the fraction of collector surface still available for deposition of particles. A variety of physicochemical and hydrodynamic factors influence the dynamic blocking function, including the chemical surface characteristics of colloids and collectors,[52] solution chemistry,[53] flow intensity,[54] particle size and shape,[30] and collector geometry.[55]

Theoretical models describing the dynamics of colloid deposition have been developed for single layer coverage of collector surfaces,[22,23,49-51,56] when repulsive electrostatic surface forces prevent interparticle contact, and for multilayer coverage.[24,48,50,57] Many particle deposition processes occurring in aqueous media are restricted to single layer (monolayer) coverage of collector surfaces, because of the prevalence of repulsive interparticle electrostatic forces that prevent contact of particles. Also a characteristic of particle deposition in aqueous media is strong attachment of particles to collectors when each carries an opposite surface charge. This high affinity between particles and collectors produces deposition that is essentially irreversible in the sense that surface diffusion and particle detachment are insignificant, as long as the prevailing hydrodynamic flow conditions and solution chemistry are maintained. When particle deposition is irreversible and restricted to monolayer coverage, the *random sequential adsorption* (RSA) mechanism may be used to describe the nonequilibrium deposition of colloids.[46]

The RSA mechanism is a nonequilibrium model based on random, irreversible deposition of particles onto stationary surfaces. Monolayer coverage and irreversibility are maintained in RSA mechanics by prohibiting particle contact, surface diffusion, and surface detachment. The most notable difference between equilibrium processes such as molecular adsorption and nonequilibrium processes typified by RSA mechanics is to be found in the packing configuration of the respective monolayers. Equilibrium conditions imply reversible attachment of particles and the attainment of close-packed configurations having a monolayer surface coverage of 90.7%.[58] This is in contrast to nonequilibrium conditions, where irreversible deposition restricts the maximum attainable monolayer density to only 54.6% coverage of the collector surface, often referred to as the *hard sphere jamming limit*.[8,59]

Despite the obvious difference between reversible processes like molecular adsorption and irreversible particle deposition, the dynamic blocking function used in most dynamic particle deposition models[22-24,48,50,51,56] is identical to the one used in the Langmuir molecular adsorption model.[60] Because it was originally designed to consider coverage of crystalline lattice sites by point-size molecules where no lateral interaction or exclusion occurs between adjacent sites, the Langmuirian blocking function does not adequately account for areal exclusion effects introduced by much larger colloidal particles. Schaaf and Talbot[61] recognized this deficiency in the Langmuir model and introduced a dynamic blocking function based on RSA mechanics that considers surface exclusion effects of particles. The RSA dynamic blocking function is applicable to models involving irreversible deposition and monolayer coverage of collector surfaces. It has a nonlinear power law dependence on surface coverage whereas the Langmuirian blocking function is linearly dependent on surface coverage.

Adamczyk *et al.*[49,62] were the first to incorporate a dynamic blocking function derived from RSA mechanics into a dynamic deposition model. Their model is restricted to a limited number of processes involving stagnation point flow hydrodynamics and colloidal deposition onto flat surfaces. For the more relevant processes involving deposition of colloids onto spherical collectors, no attempt has yet been made to incorporate an RSA-derived blocking function into a dynamic deposition model. Privman *et al.*[48] presented a dynamic particle deposition model for packed beds that utilizes a linear Langmuirian blocking function for determining both monolayer and multilayer deposition of colloids. Song and Elimelech[50,51] recognized the nonlinear nature of deposition in packed beds by extending the results of Privman *et al.* for monolayer coverage to include nonuniform deposition resulting from spherical collector geometry and surface heterogeneities. At this time, it has yet to be demonstrated whether a nonlinear dynamic blocking function based on RSA

(37) Rajagopalan, R.; Kim. J. S. *J. Colloid Interface Sci.* **1981**, *83*, 428.
(38) Dabros, T.; van de Ven, T. G. M. *Colloid Polym. Sci.* **1983**, *261*, 694.
(39) Chari, K.; Rajagopalan, R. *J. Chem. Soc. Faraday Trans. 2* **1985**, *81*, 1345.
(40) Ruckenstein, E.; Prieve, D. C. *J. Chem. Soc. Faraday Trans.* **1973**, *69*, 1522.
(41) Prieve, D. C.; Ruckenstein, E. *AIChE J.* **1974**, *20*, 1178.
(42) Rajagopalan, R.; Tien, C. *Canadian J. Chem. Eng.* **1977**, *55*, 246.
(43) Elimelech, M. *J. Colloid Interface Sci.* **1994**, *164*, 190.
(44) Elimelech, M. *Sep. Technol.* **1994**, *4*, 186.
(45) Adamczyk, Z. *Colloids Surf.* **1989**, *39*, 1.
(46) Widom, B. *J. Chem. Phys.* **1966**, *44*, 3888.
(47) Schaaf, P.; Talbot, J. *Phys. Rev. Lett.* **1989**, *62*, 175.
(48) Privman, V.; Frisch, H. L.; Ryde, N.; Matijevic, E. *J. Chem. Soc. Faraday Trans.* **1991**, *87*, 1371.
(49) Adamczyk, Z.; Siwek, B.; Zembala, M. *Colloids Surf.* **1992**, *62*, 119.
(50) Song, L.; Elimelech, M. *Colloids Surf. A* **1993**, *73*, 49.
(51) Song, L.; Elimelech, M. *J. Colloid Interface Sci.* **1994**, *167*, 301.
(52) Adamczyk, Z.; Siwek, B.; Zembala, M. *J. Colloid Interface Sci.* **1992**, *151*, 351.
(53) Adamczyk, Z.; Zembala, M.; Siwek, B.; Warszynski, P. *J. Colloid Interface Sci.* **1990**, *140*, 123.
(54) Dabros, T.; van de Ven, T. G. M. *Colloids Surf. A* **1993**, *75*, 95.
(55) Adamczyk, Z.; Belouschek, P. *J. Colloid Interface Sci.* **1991**, *146*, 123.
(56) Ruckenstein, E.; Marmur, A.; Gill, W. N. *J. Colloid Interface Sci.* **1977**, *61*, 183.
(57) Ryde, N.; Kihira, H.; Matijevic, E. *J. Colloid Interface Sci.* **1992**, *151*, 421.
(58) Graton, L. C.; Fraser, H. J. *J. Geol.* **1935**, *43*, 785.
(59) Hinrichsen, E. L.; Feder, J.; Jossang, T. *J. Statistical Phys.* **1986**, *44*, 793.
(60) Langmuir, I. *J. Am. Chem. Soc.* **1918**, *40*, 1361.
(61) Schaaf, P.; Talbot, J. *J. Chem. Phys.* **1989**, *91*, 4401.
(62) Adamczyk, Z.; Siwek, B.; Zembala, M.; Belouschek, P. *Adv. Colloid Interface Sci.* **1994**, *48*, 151.

mechanics is better than the linear Langmuirian dynamic blocking function for characterizing deposition of colloids in granular porous media.

Because there are numerous natural and technological processes involving the deposition of colloids onto spherical collectors in packed beds, our goal is to provide an improved dynamic deposition model for granular porous media. The model presented in this paper includes a dynamic blocking function based on RSA mechanics, and does not require the use of optimization or curve-fitting techniques when model parameter values are being obtained. The model is designed to generate output based on either the Langmuirian or RSA dynamic blocking function so that the usefulness of the two blocking functions may be compared. The utility of the dynamic deposition model and the superiority of the RSA blocking function are demonstrated by comparing theoretical predictions to experimental data of particle deposition dynamics in porous media obtained over a wide range of ionic strengths.

2. Theory

The theoretical model will be developed specifically for cases involving irreversible monolayer particle deposition in packed columns. It is assumed that uniform spherical collectors form the column packing material and that particle suspensions are comprised of monodisperse colloids. Hydrodynamic conditions are restricted to vertical, one-dimensional laminar flow.

2.1 The Advection–Dispersion Equation for Colloids. When characterizing the spatial and temporal variations in suspended particle concentration, the *advection–dispersion equation* is generally invoked. For an aqueous suspension of monodisperse particles flowing vertically through a packed column of spherical collectors, the one-dimensional form of the advection–dispersion equation may be utilized:[2,22,51,63]

$$\frac{\partial n}{\partial t} = D_h \frac{\partial^2 n}{\partial z^2} - v_p \frac{\partial n}{\partial z} - \frac{f}{\pi a_p^2} \frac{\partial \theta}{\partial t} \quad (1)$$

where n is the number concentration of colloidal particles in aqueous suspension, t is the time, z is the vertical spatial coordinate, and θ is the fraction of collector surface covered by deposited particles.

The first term on the right hand side of eq 1 accounts for colloidal dispersion in a porous medium, where D_h is the hydrodynamic dispersion coefficient. Hydrodynamic dispersion is generally of only minor significance in advection-dominated systems such as vertical flow through packed columns of large, sand-sized granules. As a consequence, the dispersion term is customarily omitted from eq 1 under these conditions.[2,48,50,51,64]

The advection term, the second term on the right hand side of eq 1, characterizes particle entrainment by the traveling fluid medium. Because particles generally travel slightly faster within a porous medium than the average fluid velocity,[65–70] an independent equation is required for determining the interstitial particle velocity (v_p). The particle velocity within a porous medium has been shown to be a function not only of the fluid approach velocity (U) and porosity (ϵ), but also particle radius (a_p) and average pore radius (r_0).[71–74] DiMarzio and Guttman[75] derived an expression based on these parameters for the interstitial particle velocity:

$$v_p = \frac{U}{\epsilon}\left[2 - \left(1 - \frac{a_p}{r_0}\right)^2\right] \quad (2)$$

For a porous medium comprised of uniform-sized spherical collectors, the average pore radius (r_0) can be related to the collector grain radius (a_c) by geometrical principles.[58,59] By treating the porous medium as a bundle of capillary tubes,[76] the average pore radius of an individual capillary corresponds to the radius of the "hole" occurring in the interstitial area between neighboring collector grains. Recognizing that the framework of a granular porous medium is in essence a repetitive array of rigid grains extending indefinitely in all directions, the pore radius (r_0) may be determined from the geometry of the granular packing arrangement. The granular framework consists of a mixture of cubic close-packed (ccp) and hexagonal close-packed (hcp) collector grains. In a layer of hexagonally close-packed spherical collectors, the centers of three mutually adjacent grains form an equilateral triangle, with the interstitial hole occurring at the center of the grains. A hexagonally close-packed array represents the most compact configuration of grains, having a porosity of only 25.96% and an interstitial pore radius of 0.155 times the collector radius.[58] When collector grains are arrayed in a cubic close-packing arrangement, the interstitial hole occurs at the center of four mutually adjacent grains forming a square. Cubic close-packing represents the least compact packing arrangement of grains, having a porosity of 47.60% and an interstitial pore radius of 0.414 times the collector radius.[58] Because a porous medium consists of a combination of ccp and hcp collector arrangements with an average porosity related to the ratio of the two packing arrangements, the average pore radius of the porous medium (r_0) may be interpolated between the extreme values of $0.155a_c$ and $0.414a_c$ using the average bed porosity (ϵ). That is,

$$r_0 = (1.1969\epsilon - 0.1557)a_c \quad (3)$$

The particle deposition term occurs last in sequence on the right hand side of eq 1. The kinetics of the deposition process are included in this term by the rate expression for fractional surface coverage ($\partial\theta/\partial t$). The fractional surface coverage (θ) quantifies the relative amount of collector surface area covered by deposited particles. At the *jamming limit* (θ_{max}), the maximum coverage of collector surfaces has been attained.

Lastly, the variable f in eq 1 represents the specific surface area of the porous medium, *i.e.* the collector surface area per unit volume of packed bed. For a packed bed of uniform spherical collectors, it is given by[48,50]

$$f = \frac{3(1-\epsilon)}{\epsilon a_c} \quad (4)$$

Before the advection–dispersion equation (eq 1) can be solved, an independent equation must be obtained for the

(63) Bear, J. *Dynamics of Fluids in Porous Media;* Dover Publications: New York, 1972.
(64) Rajagopalan, R.; Adin, A. *J. Environ. Eng., ASCE* **1989**, *115*, 785.
(65) Wood, W. W.; Ehrlich, G. G. *Ground Water* **1978**, *16*, 398.
(66) Smith, M. S.; Thomas, G. W.; White, R. E.; Ritonga, D. *J. Environ. Qual.* **1985**, *14*, 87.
(67) Enfield, C. G.; Bengtsson, G. *Ground Water* **1988**, *26*, 64.
(68) Matthess, G.; Pekdeger, A.; Schroeter, J. *J. Contam. Hydrol.* **1988**, *2*, 171.
(69) Harvey, R. W.; George, L. H.; Smith, R. L.; LeBlanc, D. R. *Environ. Sci. Technol.* **1989**, *23*, 51.
(70) Toran, L.; Palumbo, A. V. *J. Contam. Hydrol.* **1992**, *9*, 289.
(71) Small, H. *J. Colloid Interface Sci.* **1974**, *48*, 147.
(72) Stoisits, R. F.; Poehlein, G. W.; Vanderhoff, J. W. *J. Colloid Interface Sci.* **1976**, *57*, 337.
(73) Prieve, D. C.; Hoysan, P. M. *J. Colloid Interface Sci.* **1978**, *64*, 201.
(74) Silebi, C. A.; DosRamos, J. G. *J. Colloid Interface Sci.* **1989**, *130*, 14.
(75) DiMarzio, E. A.; Guttman, C. M. *Macromolecules* **1970**, *3*, 131.
(76) Taylor, G. I. *Proc. Roy. Soc. A* **1953**, *219*, 186.

rate expression $\partial\theta/\partial t$. The expression used for $\partial\theta/\partial t$ is a kinetic rate equation that accounts for deposition dynamics as well as kinetics. The kinetic rate equation must be solved in conjunction with the advection–dispersion equation to obtain the spatial and temporal variations in suspended particle concentration for fluid flow in a porous medium.

2.2 Rate Equation for Fractional Surface Coverage. When solution and surface conditions restrict particle deposition on collector surfaces to monolayer coverage, the following rate equation is used to characterize deposition dynamics:[48,50,60,61]

$$\frac{\partial\theta}{\partial t} = \alpha K \pi a_p^2 n B(\theta) \tag{5}$$

where α is the particle attachment (collision) efficiency, K is the particle transfer coefficient, and $B(\theta)$ is the *dynamic blocking function*.

The attachment efficiency (α) represents the fraction of particle collisions with collector surfaces resulting in attachment.[33,48,50] When colloidal particles and collector surfaces have opposite charges, essentially all collisions result in particle attachment because of the strong attractive energy between particles and collectors. Under these conditions, deposition is said to be favorable, and a value of 1 may be used for α.

The particle transfer coefficient (K) characterizes the kinetics of capture of suspended colloidal particles by bare collector surfaces in a packed bed. When attractive double layer forces exist between particles and collectors, K exhibits sensitivity to solution chemistry and hydrodynamic conditions.[34,43,44] The particle transfer coefficient (K) is obtained from the fluid approach velocity (U) and the single collector efficiency (η) using[2,41,50]

$$K = \frac{\eta U}{4} \tag{6}$$

Rigorous determination of the single collector efficiency (η) when colloidal and hydrodynamic interactions are considered requires a numerical solution of the convective diffusion equation for flow around spherical collectors. The method outlined in Elimelech and Song[77] was used in this study for obtaining η. This method utilizes Happel's sphere-in-cell flow model[78–80] for obtaining the flow field around spherical collectors in a packed bed and a finite difference numerical scheme for determining the colloidal deposition rate as a function of solution chemistry and hydrodynamic conditions.

The dynamic blocking function $B(\theta)$ characterizes the dynamic (transient) nature of the particle deposition rate. A dynamic deposition rate arises as particles accumulate on collector surfaces, thereby excluding a portion of the surface from subsequent particle attachment. This results in a declining probability that approaching particles will impact an unoccupied site on the collector surface as deposition proceeds. The dynamic blocking function is designed to represent this changing probability as a function of fractional surface coverage (θ). For initially bare (particle-free) collector surfaces, $B(\theta) = 1$. As deposited particles begin to block surface sites from further deposition, $B(\theta)$ decreases until the jamming limit is reached (*i.e.* $\theta = \theta_{max}$) at $B(\theta) = 0$. Separate mathematical expressions are available for the dynamic blocking function, based on either the Langmuir adsorption model or RSA mechanics.

2.3 The Langmuirian Dynamic Blocking Function. The Langmuirian dynamic blocking function is identical to the linear blocking function described in Langmuir's molecular adsorption model.[60] It displays a linear dependence on fractional surface coverage (θ), such that

$$B(\theta) = \frac{\theta_{max} - \theta}{\theta_{max}} = 1 - \beta\theta \tag{7}$$

where β is the *excluded area parameter*, equivalent to the reciprocal of the jamming limit (θ_{max}). The excluded area parameter is a measure of the collector surface area blocked from subsequent deposition by a deposited particle. It is expressed as a dimensionless quantity determined by the ratio of the blocked surface area to the projected (cross-sectional) area of retained particles. A method for obtaining β from experimental particle breakthrough curves is presented in a subsequent section.

The Langmuirian dynamic blocking function was originally intended to address surface exclusion of crystalline lattice sites by point-size molecules, where areal (two-dimensional) blocking is insignificant. As a consequence, the Langmuirian dynamic blocking function does not adequately describe surface exclusion effects of larger colloidal particles which individually block numerous lattice points.[61] For deposition of colloids, the relationship between blocking and fractional surface coverage is no longer described by a linear relationship, and surface exclusion effects demand the use of a more sophisticated blocking function. A nonlinear dynamic blocking function based on RSA mechanics that addresses surface exclusion effects is presented below.

2.4 The RSA Dynamic Blocking Function. When stable colloidal particles deposit onto oppositely charged collector surfaces, the following conditions should apply:[46] (i) attachment is irreversible as long as chemical and hydrodynamic conditions are maintained, (ii) surface diffusion is negligible, and (iii) particle–particle contact is prohibited. Under these conditions, the RSA mechanism is directly applicable and may be used to obtain a dynamic blocking function for colloidal particles.

Schaaf and Talbot[47,61] developed a dynamic blocking function from the RSA mechanism that applies to deposition of noninteracting (hard) spheres onto flat collector surfaces. Their blocking function is based on a virial expansion of excluded area effects to the third order in density and may be used for low and moderate surface coverage:[61]

$$B(\theta) = 1 - 4\theta + \frac{6\sqrt{3}}{\pi}\theta^2 + \left(\frac{40}{\sqrt{3}\pi} - \frac{176}{3\pi^2}\right)\theta^3 \tag{8}$$

This equation applies only to deposition that is subject to the hard sphere jamming limit (θ_∞). A more general expression, applicable to any collector geometry and soft particle deposition, may be obtained from eq 8 based on the jamming limit for general cases (θ_{max}). The general expression is obtained by incorporating the function $\theta_\infty\beta$ into eq 8.[49] This results in

$$B(\theta) = 1 - 4\theta_\infty\beta\theta + 3.308(\theta_\infty\beta\theta)^2 + 1.4069(\theta_\infty\beta\theta)^3 \tag{9}$$

This generalized expression for the dynamic blocking function applies to surface coverages at or below $0.8\theta_{max}$. A separate expression is necessary when surface coverage approaches the jamming limit (θ_{max}).

(77) Elimelech, M.; Song, L. *ACS Symposium Series 491*; Sabatini, D. A., and Knox, R. C., Eds.; American Chemical Society, Washington, DC, 1992.
(78) Happel, J. *AIChE J.* **1958**, *4*, 197.
(79) Song, L.; Elimelech, M. *J. Colloid Interface Sci.* **1992**, *153*, 294.
(80) Pfeffer, R.; Happel, J. *AIChE J.* **1964**, *10*, 605.

As coverage of a flat collector surface approaches the hard sphere jamming limit, Pomeau[81] demonstrated that the RSA dynamic blocking function becomes

$$B(\theta) = \frac{(\theta_\infty - \theta)^3}{2k^2} \tag{10}$$

where k is the jamming limit slope, with a value determined by Hinrichsen *et al.*[59] to be 0.236 for hard spheres depositing on flat surfaces (*i.e.* $\theta_{max} = \theta_\infty$). Pomeau's expression (eq 10) may be generalized to account for soft particle interactions by substituting θ_{max} for θ_∞:

$$B(\theta) = \frac{(\theta_{max} - \theta)^3}{2k^2} = \frac{(1 - \beta\theta)^3}{2k^2\beta^3} \tag{11}$$

This modified expression for the dynamic blocking function applies when surface coverage is in excess of $0.8\theta_{max}$. The jamming limit slope k is no longer a constant value in the modified expression and must be independently determined for differing solution chemistry and hydrodynamic conditions (see next subsection for procedural details). Pomeau's modified expression for blocking near the jamming limit (eq 11) is to be utilized in conjunction with Schaaf and Talbot's modified dynamic blocking function (eq 9) when incorporating an RSA-derived blocking function into the kinetic rate equation (eq 5) for characterization of deposition dynamics.

2.5 Determining the Excluded Area Parameter for a Porous Medium. Utilization of either blocking function (Langmuirian or RSA) as part of the kinetic rate equation requires a means of determining the excluded area parameter (β). The area of collector surface excluded by a particle from further deposition depends on a complex variety of physicochemical and hydrodynamic factors, including solution chemistry, surface chemistry, geometry and size of particles and collectors, and flow conditions. Expressions for determining the excluded area parameter *a priori* exist only for the simplest flow conditions and collector geometry, *i.e.* stagnation point flow and flat collector surfaces.[52] For more complex systems, such as spherical collectors in packed beds, the excluded area parameter must be determined from experimental data. A technique is presented based on the evolution of collector surface coverage near the jamming limit. This procedure yields a value for the excluded area parameter from experimental particle breakthrough data.

Pomeau[81] and Swendsen[82] have examined irreversible monolayer deposition near the jamming limit, demonstrating a power law relationship between fractional surface coverage and time in the form of

$$\theta_{max} - \theta = kt_d^{-1/2} \tag{12}$$

where t_d is a dimensionless quasi-time variable referred to as the porous medium deposition time.[52] The deposition time is a measure of the cumulative number of attempts made at depositing particles on a unit area of collector surface.[55,59] For a granular porous medium subject to excluded area effects associated with irreversible, monolayer particle deposition, the deposition time t_d is determined from[52,55]

$$t_d = \frac{K\pi a_p^2}{\theta_{max}} \int_0^t n \, dt \tag{13}$$

Since the jamming limit (θ_{max}) is not known *a priori*, the hard sphere jamming limit value of 0.546 may be used to obtain an initial estimate of t_d. Equations 12 and 13 are used along with experimental particle breakthrough curve data to obtain values for the jamming limit slope (k) and the jamming limit (θ_{max}). The value obtained for the jamming limit is then used to replace 0.546 in eq 13 so that an updated estimate of t_d may be determined. Values for the fractional surface coverage (θ) as required by eq 12 are also obtained from particle breakthrough curves using[50]

$$\theta = \frac{\pi a_p^2 U a_c n_0 \int_0^t (1 - n/n_0)\, dt}{3L(1 - \epsilon)} \tag{14}$$

where L is the length of the packed column and n_0 is the inlet particle concentration to the column. As t_d becomes large, a plot of θ vs $t_d^{-1/2}$ asymptotically approaches a straight line. By fitting a straight line to the linear portion of the data, the slope of the line yields the jamming limit slope (k) and the intercept value corresponds to the jamming limit (θ_{max}). The value for k is required by the RSA dynamic blocking function for high surface coverage, as previously discussed. The excluded area parameter β is readily obtained from the experimentally determined value for θ_{max}, *i.e.*,

$$\beta = \frac{1}{\theta_{max}} \tag{15}$$

2.6 Governing Equations and Numerical Solution. The governing equations forming the basis of the dynamic deposition model are the advection–dispersion equation (eq 1) and the kinetic rate equation (eq 5). These equations are coupled through the rate expression for fractional surface coverage $\partial\theta/\partial t$. Simultaneous solution of the coupled governing equations will produce theoretical particle breakthrough curves when the following initial and boundary conditions are applied:

$$n(z,0) = 0 \tag{16a}$$

$$n(0,t>0) = n_0 \tag{16b}$$

$$\theta(z,0) = 0 \tag{16c}$$

$$\theta(z,t\to\infty) = \theta_{max} \tag{16d}$$

Simultaneous solution of eqs 1 and 5 subject to the above boundary and initial conditions requires the use of either finite difference or finite element numerical techniques. When experimental conditions allow it, as in our case involving one-dimensional advection-dominated flow through a packed bed of coarse-grained material, the dispersion term is omitted from eq 1. This greatly facilitates the solution procedure by allowing the transformation of the coupled governing equations (*i.e.* eqs 1 and 5) to the so-called breakthrough coordinates.[48,50,51] The following transformations are performed according to the method described in Privman *et al.*:[48]

$$x = \frac{z}{v_p} \tag{17a}$$

$$\tau = t - \frac{z}{v_p} \tag{17b}$$

Following these transformations, the coupled governing

(81) Pomeau, Y. *J. Phys. A: Math. Gen.* **1980**, *13*, L193.
(82) Swendsen, R. H. *Phys. Rev. A* **1981**, *24*, 504.

Table 1. Physical and Chemical Conditions Used in the Packed Bed Particle Deposition Experiments

condition	description	condition	description
particle type	latex particles	electrokinetic (ζ_p) potential of particles	38.1 (low I) to 8.9 mV (high I)
surface functional groups	amidine (-NH_3+)	electrokinetic (ζ_c) potential of collectors	−38.8 (low I) to −7.8 mV (high I)
particle radius, a_p	0.239 μm	influent particle concentration, n_0	2.49×10^{14} m^{-3} (14.9 mg/L)
particle density	1.055 g/cm^3	approach velocity, U	0.1 cm/s
collector type	soda-lime glass beads	bed depth, L	10 cm
collector radius, a_c	0.23 mm	bed porosity, ϵ	0.359
ionic strength, I	from 6×10^{-6} to 10^{-1} M KCl	temperature	25 °C
solution pH	5		

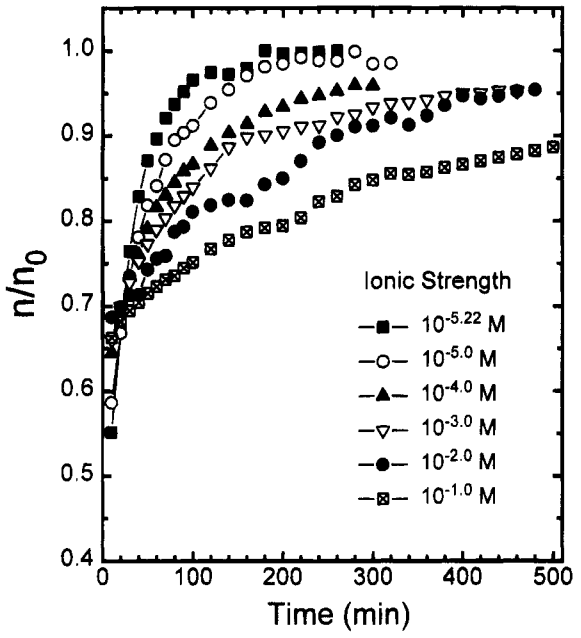

Figure 1. Experimental particle breakthrough curves at different solution ionic strengths. Experiments were conducted under the conditions summarized in Table 1.

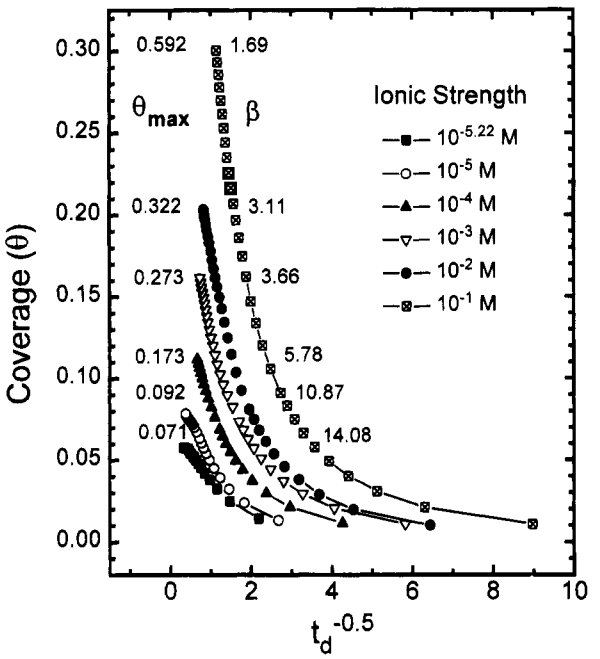

Figure 2. Determining the excluded area parameter from the experimental data shown in Figure 1. The values of θ_{max} are determined by extrapolating the linear portion of each curve to the vertical intercept. The parameter β is the reciprocal value of θ_{max}. The slope of the linear portion of each curve corresponds to the jamming limit slope (k).

equations assume the following form:

$$\frac{\partial n}{\partial x} + \alpha K f n B(\theta) = 0 \tag{18a}$$

$$\frac{\partial \theta}{\partial \tau} - \alpha K \pi a_p^2 n B(\theta) = 0 \tag{18b}$$

The transformed initial and boundary conditions are

$$n(x,0) = 0 \tag{19a}$$

$$n(0,\tau>0) = n_0 \tag{19b}$$

$$\theta(x, 0) = 0 \tag{19c}$$

$$\theta(x,\tau\rightarrow\infty) = \theta_{max} \tag{19d}$$

which correspond to a step input of suspended colloidal particles and initially clean collector surfaces.

The procedure used to solve the transformed governing equations (eqs 18a and 18b) will vary, depending on whether the Langmuirian (eq 7) or the RSA dynamic blocking functions (eqs 9 and 11) are utilized. When the linear Langmuirian dynamic blocking function is incorporated into the governing equations for $B(\theta)$, an analytical solution is available. According to the procedure outlined in Kallay *et al.*[23] and Privman *et al.*,[48] the particle concentration $n(x,\tau)$ is given by

$$n(x,\tau) = \frac{n_0 \exp(\alpha K \pi a_p^2 \beta n_0 \tau)}{\exp(\alpha K \pi a_p^2 \beta n_0 \tau) + \exp(\alpha K f x) - 1} \tag{20}$$

When the nonlinear RSA blocking functions are used in the coupled governing equations, an analytical solution is no longer available. The governing equations are not independent and therefore must be solved simultaneously using an iterative numerical technique. In this case, a numerical procedure similar to that described by Song and Elimelech[50] is used to obtain values for $n(x,\tau)$.

3. Results and Discussion

3.1 Experimental Particle Breakthrough Curves. As a means of evaluating the utility of the RSA dynamic blocking function, theoretical results obtained from the dynamic deposition model are compared with experimental particle breakthrough curves. The particle breakthrough curves were collected under irreversible deposition conditions using an aqueous suspension of positively charged latex colloids and a packed column of negatively charged glass beads. These column experiments were conducted over a wide range of ionic strengths while maintaining constant physical and hydrodynamic conditions. A summary of the physicochemical and hydrodynamic parameters maintained in the experiments is provided in Table 1. The set of experimentally generated particle breakthrough curves to be analyzed in the ensuing

subsections is shown in Figure 1. Additional details of the particle deposition experiments are provided elsewhere.[83,84]

3.2 The Excluded Area Parameter. Excluded area parameter values were derived from the experimental particle breakthrough curves shown in Figure 1 by using the procedure described in subsection 2.5. Plots of the fractional surface coverage (θ) as a function of $t_d^{-1/2}$ for each ionic strength used in the deposition experiments are presented in Figure 2, along with the calculated value for the jamming limit (θ_{max}) and the corresponding value for the excluded area parameter (β) (recall that $\theta_{max} = 1/\beta$). The set of plots portrayed in Figure 2 effectively illustrates the sensitivity exhibited by β to changes in ionic strength. A steady decline in β is noted as ionic strength is increased, in qualitative agreement with DLVO theory,[85,86] as well as with previous experimental investigations involving irreversible monolayer deposition of colloids onto flat surfaces.[30,49,55] Classical DLVO theory states that an increase in ionic strength causes a compression of the electrical double layer surrounding charged particle surfaces. Double layer compression produces a corresponding reduction in the effective range of repulsive interaction between similarly charged particles, thereby reducing the area of exclusion exerted by a deposited particle on the surface of a collector.

According to RSA mechanics, the minimum value of β attainable for stable particles undergoing irreversible monolayer deposition is 1.83, the reciprocal value of the hard sphere jamming limit.[54] Values of β in excess of 1.83 are an indication of either "soft sphere" particle deposition or nonstagnation point flow conditions, whereas values below 1.83 are in violation of RSA mechanics and must therefore be attributed to colloidal instability. Soft sphere deposition occurs whenever electrostatic repulsion prevents hard sphere contact of particles. The electrostatic energy barrier between particles produces an effective (soft sphere) radius larger than the actual (hard sphere) radius, resulting in an excluded area that is larger than 1.83.

A plot of the experimentally derived β values as a function of ionic strength is presented in Figure 3. The reciprocal hard sphere jamming limit value of 1.83 represents the transition point from stable particles undergoing monolayer deposition to particle instability and multilayer deposition. The logarithmic decline of β as a function of ionic strength noted in the stable, monolayer region above $\beta = 1.83$ is a reflection of electrical double layer compression or particle "hardening". The β value of 1.69 at an ionic strength of 0.1 M is an indication of multilayer deposition of unstable particles resulting from total collapse of the electrostatic energy barrier necessary for maintaining colloidal stability.

For spherical collectors, the value of the hard sphere jamming limit will differ from 0.546, the value determined for stagnation point flow of particles onto flat surfaces.[59] In addition, nonstagnation point flow produces an excluded area parameter that is position-dependent and specific for a given set of physicochemical and hydrodynamic conditions. Nonstagnation point flow conditions result when the incidence angle between fluid trajectories and the collector surface deviates from 90°. The tangential, or shear, component of the fluid trajectory creates a

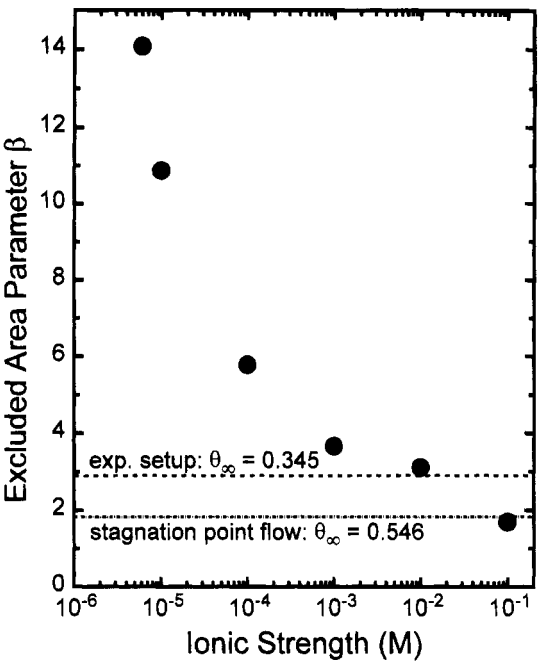

Figure 3. Determining the hard sphere jamming limit for spherical collectors in a packed bed. The asymptotic limit for β of 2.9 corresponds to a hard sphere jamming limit (θ_∞) of 0.345 for the spherical collector configuration utilized in the experimental setup. This value is unique for the hydrodynamic and physical conditions outlined in Table 1.

"shadow zone" on the collector surface downgradient of a deposited particle where the probability of subsequent deposition is reduced by the so-called "hydrodynamic scattering effects".[87] On a spherical collector surface, the area of the shadow zone increases as fluid shear increases, resulting in a position-dependent value for the excluded area parameter. The forward and rear stagnation points are the only locations on a spherical collector not subject to hydrodynamic scattering effects whereas the region midway between the stagnation points will experience the largest shadow zone. Because of the dependence of the excluded area parameter on angular position, experimentally determined β values represent a spatial average of the entire collector surface. The average excluded area parameter for packed beds of spherical particles will vary, depending on solution ionic strength, flow rate, surface characteristics, and the ratio between particle size and collector size.[87-89]

For spherical collectors and a given set of physicochemical and hydrodynamic conditions, a unique value for the hard sphere jamming limit may be determined for a porous medium from β values collected over a wide range of ionic strengths. As the ionic strength is increased to the point where particle aggregation is initiated, the excluded area parameter asymptotically approaches a minimum limiting value (*e.g.* for ionic strength smaller than 0.1 M in Figure 3) corresponding to the reciprocal of the hard sphere jamming limit. The asymptotic limit of $\beta = 2.9$ noted in Figure 3 relates to a hard sphere jamming limit value of 0.345, which is specific to spherical collector geometry and the experimental conditions outlined in Table 1. This value represents an area-averaged composite of localized jamming limit values taken across the entire collector surface. Because nonstagnation point

(83) Liu, D. Unpublished Ph.D. Dissertation. University of California, Los Angeles, 1994.
(84) Liu, D.; Johnson, P. R.; Elimelech, M., submitted.
(85) Derjaguin, B. V.; Landau, L. D. *Acta Physicochim.* **1941**, *14*, 633.
(86) Verwey, E. J. W.; Overbeek, J. T. G. *Theory of the Stability of Lyophobic Colloids;* Elsevier: Amsterdam, 1948.
(87) Adamczyk, Z.; Siwek, B.; Szyk, L.; Zembala, M. *Bull. Polish Acad. Sci. Chem.* **1993**, *41*, 41.
(88) Dabros, T. *Colloids Surf.* **1989**, *39*, 127.
(89) Dabros, T.; van de Ven, T. G. M. *J. Colloid Interface Sci.* **1992**, *149*, 493.

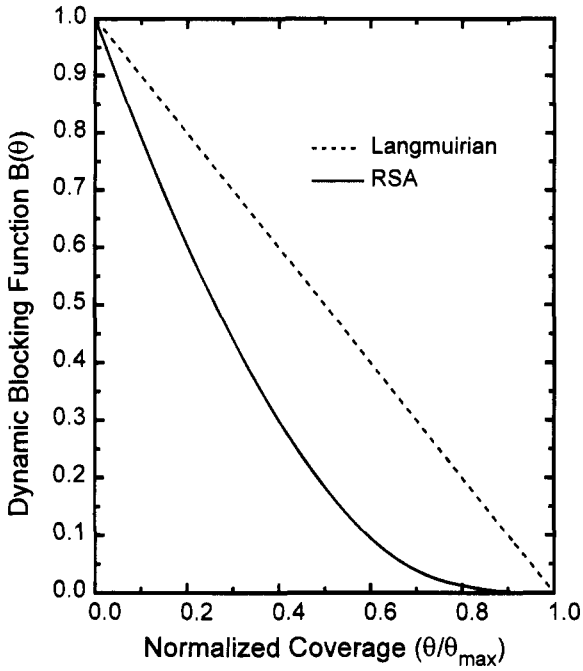

Figure 4. Comparison of dynamic blocking functions as a function normalized fractional surface coverage based on the Langmuir model and RSA mechanics. Values of 1.83 and 0.236 were used for β and k, respectively.

flow produces hydrodynamic scattering effects that reduce the surface area available for deposition, the hard sphere jamming limit for spherical collectors will always be less than 0.546 (corresponding to $\beta > 1.83$).

3.3 Comparison of Dynamic Blocking Functions. Separate dynamic blocking functions based on the Langmuir model and RSA mechanics are displayed in Figure 4. Curves for the blocking functions were generated from eqs 7, 9, and 11 using standard parameter values of 1.83 for β and 0.236 for k. For purposes of comparison, the blocking functions are plotted against normalized fractional surface coverage (θ/θ_{max}).

The RSA dynamic blocking function exhibits a variety of distinguishing characteristics not found in the Langmuirian dynamic blocking function. Most notable is its nonlinearity with respect to fractional surface coverage. This is a reflection of the third order power law dependence of blocking on surface coverage, a characteristic not found in the Langmuir model.

A quantitative comparison of the dynamic blocking functions presented in Figure 4 reveals that for any fractional surface coverage, the RSA dynamic blocking function value is less than the comparable value for the Langmuirian dynamic blocking function. This suggests that the effects of particle blocking on the dynamics of particle deposition will be more profound when the RSA blocking function is used in lieu of the Langmuirian blocking function. Note that the value for the RSA dynamic blocking function has fallen near zero at 80% surface coverage whereas the corresponding value for the Langmuirian dynamic blocking function has been reduced to 0.2. Thus, the RSA mechanism predicts greatly reduced rates of deposition during the early stages and very little late stage deposition as the jamming limit is approached, whereas a steady decline in deposition is indicated by the Langmuir model for the entire range of surface coverage.

Other differences between the respective blocking functions are revealed by their slopes. A faster rate of blocking during the early stages of deposition is indicated by the initially steeper slope of the RSA dynamic blocking

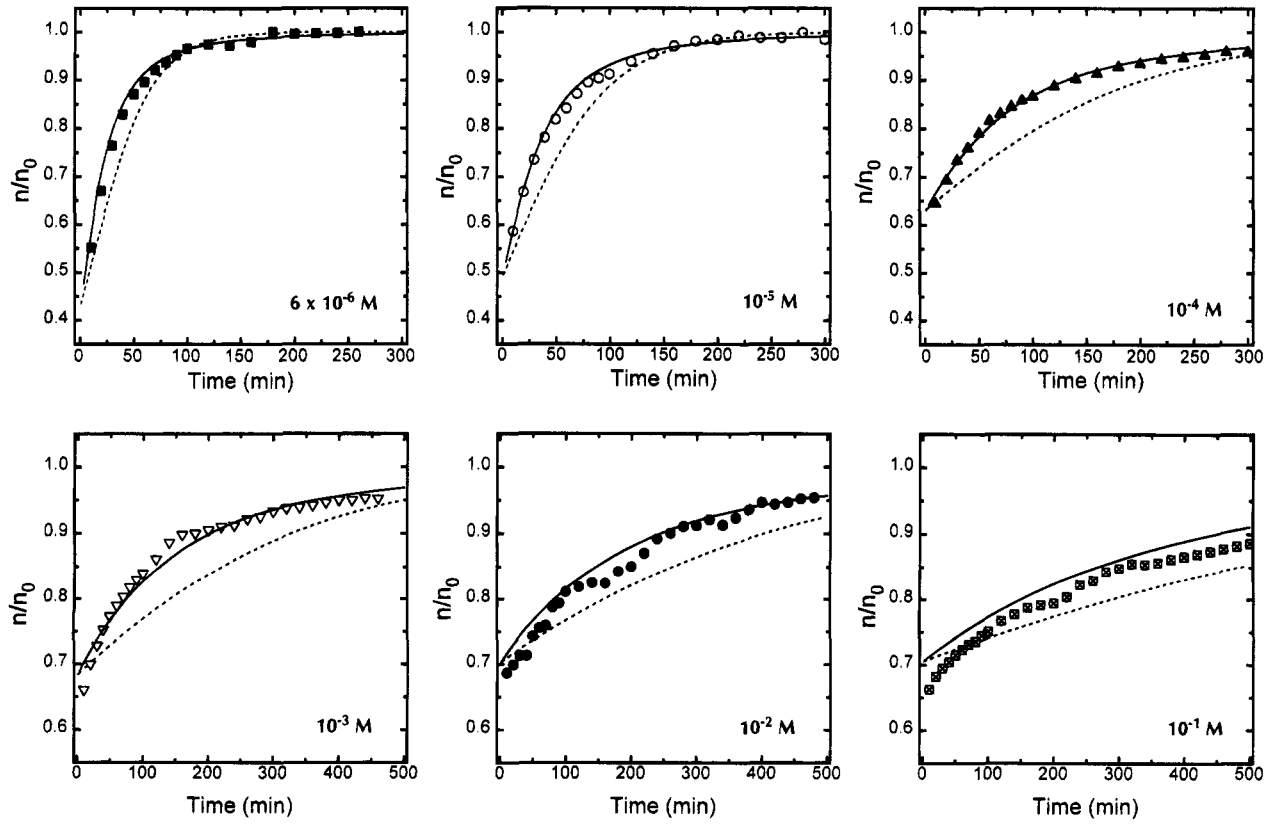

Figure 5. Comparison of experimental and theoretical particle breakthrough curves based on Langmuirian and RSA blocking functions. Experimental conditions and parameter values used in the theoretical model are summarized in Tables 1 and 2. Solid curves represent theoretical breakthrough curves based on the RSA blocking function whereas dashed curves correspond to theoretical curves based on the Langmuirian blocking function. Experimental breakthrough data points for each ionic strength were taken from Figure 1.

Table 2. Values of Calculated Parameters Used in the Theoretical Model

ionic strength (M)	excluded area parameter (β)	jamming limit slope (k)	particle transfer coefficient (K) (m/s)
6×10^{-6}	14.08	0.033	1.00×10^{-6}
10^{-5}	10.87	0.037	8.41×10^{-7}
10^{-4}	5.78	0.092	5.52×10^{-7}
10^{-3}	3.66	0.152	4.55×10^{-7}
10^{-2}	3.11	0.143	4.21×10^{-7}
10^{-1}	1.69	0.256	4.17×10^{-7}

function. This initial steepness is manifested in terms of its effect on theoretical particle breakthrough curves as a steeper initial rise in particle concentration. As surface coverage progresses, the declivity of the RSA blocking function is gradually diminished to the point of flatness, whereas the Langmuirian blocking function slope remains constant. This suggests a diminishing rate of change in particle deposition as reflected in the RSA mechanism, a transient characteristic not reflected in the Langmuir model. The initially steeper particle breakthrough curve produced by the RSA blocking function will eventually crossover its Langmuirian counterpart as the rate of blocking declines in the later stages of deposition. The flatter slope and reduced values of the RSA blocking function near the jamming limit suggest a severely reduced but constant deposition rate during the late stages of surface coverage and a correspondingly slower approach to full monolayer coverage than what is indicated by the Langmuirian blocking function. Similar distinctions in behavior between the two dynamic blocking functions were reported by Adamczyk *et al.*[49] for stagnation point flow particle deposition onto flat surfaces.

3.4 Comparison of Experimental and Theoretical Breakthrough Curves. Theoretical model output based on both Langmuirian and RSA dynamic blocking functions are compared to the previously described experimental breakthrough curves in Figure 5. The experimental parameter values summarized in Table 1 were used in the theoretical calculations. In addition, calculated parameters as required by the model are presented in Table 2 for the ionic strengths investigated. The parameters β and k were determined from the plots shown in Figure 2 based on the method described in subsection 2.5. The particle transfer coefficient K for each ionic strength was calculated from a numerical solution of the convective diffusion equation with colloidal and hydrodynamic interactions fully incorporated.[77] Theoretical breakthrough curves based on Langmuirian blocking were obtained from eq 20, whereas breakthrough curves based on RSA blocking required the substitution of eqs 9 and 11 into eq 18 for low and high surface coverage, respectively.

An exceptional fit of the experimental breakthrough curves is clearly provided by the theoretical output based on RSA mechanics, especially for ionic strengths less than 0.1 M. This is visual proof of the superiority of the RSA mechanism as a means of quantifying the effects of surface blocking on the dynamics of particle deposition in porous media. The relatively poor fit between theory and experiment for solution ionic strength of 0.1 M is attributable to a violation of the monolayer limit as required by RSA mechanics. At high ionic strength, particles become unstable due to compression of their electrical double layers, resulting in particle contact and multilayer rather than monolayer particle deposition onto collector surfaces.

By controlling the magnitude of the excluded area parameter, the solution ionic strength plays a major role in determining the behavior of particle breakthrough in packed columns. At reduced ionic strengths (*i.e.* 6×10^{-6} M and 10^{-5} M), the RSA breakthrough curve has already crossed over the Langmuirian breakthrough curve and has nearly attained a constant value, whereas the breakthrough curves generated at higher ionic strengths have not yet crossed and are still on the rise. These differences are attributable to larger excluded areas associated with particles at reduced ionic strength, resulting in a faster rate of blocking and fewer particles required to complete a monolayer on collector surfaces.

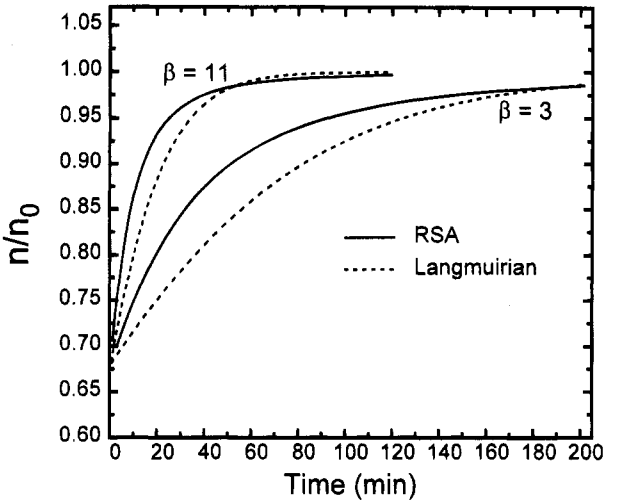

Figure 6. Theoretical particle breakthrough curves based on Langmuirian and RSA dynamic blocking functions for a short column ($L = 10$ cm) and two different values of β. The following parameters were used: $\alpha = 1$; $K = 5 \times 10^{-7}$ m/s; $n_0 = 10^{15}$ m^{-3}; $a_p = 0.25$ μm; $a_c = 0.25$ mm; $U = 0.001$ m/s.

As discussed in the previous subsection, theoretical particle breakthrough curves based on RSA blocking display a sharper initial rise in concentration and a more gradual approach toward total breakthrough than curves based on Langmuirian blocking. This has implications for future experimental studies involving particle deposition in packed beds under physicochemical conditions where blocking is important, as it indicates that much longer times are required to reach total particle breakthrough than the 1 or 2 h normally used in deposition experiments. Similar conclusions were drawn by Adamczyk and co-workers[49] for particle deposition onto flat surfaces.

It is worth noting that all parameters required by the dynamic deposition model were obtained *a priori* using known parameters (*e.g.* L, ϵ, a_p, a_c, and n_0), theoretical principles (*e.g.* K and α), or asymptotic graphical methods based on experimental data (*e.g.* β and k). No parameter optimization or curve-fitting techniques were used to obtain a closer fit between theoretical output and experimental measurements. The excellent agreement between theoretical breakthrough curves based on RSA mechanics and experimentation for the wide range of ionic strengths investigated is strong proof of the general utility of the RSA mechanism for describing irreversible monolayer deposition of colloids in granular porous media.

3.5 Particle Breakthrough Curve Simulations. In order to better evaluate the effects of solution ionic strength and porous medium depth on the deposition process, particle breakthrough was simulated for different β values and column lengths. The results for short (10 cm) and long (100 cm) columns are shown in Figures 6 and 7, respectively. Excluded area parameter values utilized in the simulations roughly correspond to ionic strengths of 10^{-2} M ($\beta = 3$) and 10^{-5} M ($\beta = 11$), values that span the range of solution conditions commonly encountered in particle deposition processes. Column lengths of

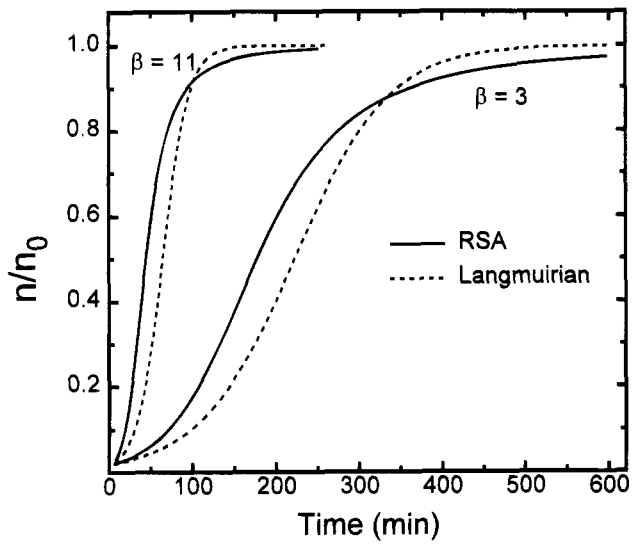

Figure 7. Theoretical particle breakthrough curves based on Langmuirian and RSA dynamic blocking functions for a long column ($L = 100$ cm) and two different values of β. The following parameters were used: $\alpha = 1$; $K = 5 \times 10^{-7}$ m/s; $n_0 = 10^{15}$ m^{-3}; $a_p = 0.25$ μm; $a_c = 0.25$ mm; $U = 0.001$ m/s.

10 and 100 cm were chosen to reflect the range of values commonly used in particle deposition studies involving packed columns. Other parameters used in the simulation are typical parameter values corresponding to favorable particle–collector interactions involving irreversible deposition and monolayer coverage.

The initial "clean" bed removal of particles is considerably less than 100% in the short column simulations (L = 10 cm, Figure 6), so normalized particle effluent concentration is well above zero at reduced time $\tau = 0$. A significant enhancement of clean bed particle removal is realized by increasing column length ($L = 100$ cm, Figure 7), with almost total removal of particles occurring at $\tau = 0$. Further qualitative observations of these simulations provide insight into the effect of blocking on the timing of particle breakthrough, as discussed below.

The solution ionic strength and particle travel distance each have a marked effect on the shape and timing of particle breakthrough curves. Large β values corresponding to reduced ionic strength result in rapid blocking of collector surfaces and earlier initial breakthrough of particles. The RSA mechanism consistently produces earlier breakthrough of particles, followed by crossover and a slower approach to the jamming limit than its Langmuirian counterpart. This is a reflection of the enhanced sensitivity of the RSA blocking function to excluded area effects exerted by deposited particles.

As column length is increased from 10 to 100 cm, particle breakthrough curves generated from both models assume the classic sigmoidal shape commonly associated with equilibrium adsorption isotherms and hydrodynamic dispersion of solutes. However, this sigmoidal shape cannot be attributed to equilibrium conditions, since the model used to generate the particle breakthrough curves shown in Figure 7 is based on nonequilibrium, irreversible particle deposition. Furthermore, hydrodynamic dispersion of particles must also be ruled out as the cause of sigmoidicity, because the dispersion term was eliminated from the model prior to transformation of the governing equations to breakthrough coordinates. The explanation for the sigmoidal shape exhibited by the simulated particle breakthrough curves resides in the actual deposition process, where the irreversibility of particle deposition onto spherical collector surfaces produces a nonlinear, sigmoidal breakthrough signature. Similar nondispersional breakthrough curves having a sigmoidal shape were generated by Song and Elimelech's[51] theoretical model involving particle deposition in porous media under unfavorable conditions subject to surface charge heterogeneities.

3.6 On the Nonlinear Dependence of Deposition Rate on Surface Coverage. The nonlinear relationship between particle deposition rate and fractional surface coverage is perhaps the most salient feature displayed by the RSA model (see Figure 4). This nonlinearity was demonstrated to be a direct result of excluded area effects exerted on collector surfaces by irreversibly deposited particles. In addition to excluded area effects, nonlinear deposition dynamics also arise when particles deposit on collector surfaces in a nonuniform fashion. The sources of nonuniform particle deposition include hydrodynamic scattering,[87–89] surface heterogeneities,[51,90] and nonuniformly accessible surfaces.[50,62]

The hydrodynamic scattering effect was shown in an earlier section to magnify the local value of the excluded area parameter by creating a shadow zone downgradient of deposited particles. For spherical collectors, the size of the shadow zone is known to vary according to solution chemistry, flow conditions, and angular position on the collector surface with respect to the stagnation points.[87–89] This dependence of hydrodynamic scattering on angular position produces nonuniform deposition on spherical collectors, which results in a nonlinear relation between deposition rate and fractional surface coverage.

Collector surfaces contain unevenly distributed nonidealities such as lattice imperfections, surface roughness, chemical impurities, and other types of charge heterogeneities known to produce nonuniform particle deposition.[51,90] In their model for transient deposition in heterogeneous porous media, Song and Elimelech[51] demonstrated that nonuniform particle deposition arising from heterogeneously charged spherical collector surfaces result in nonlinear deposition dynamics similar in nature to the nonlinearity displayed by RSA mechanics. Their model showed that particle deposition under unfavorable conditions occurs preferentially onto local, energetically favorable sites that are a minor component of an otherwise unfavorable surface. Under these conditions, the deposition rate is highly dependent on the extent of surface charge heterogeneity, and a nonlinear dependence of deposition rate on surface coverage results as locally favorable sites are rapidly exhausted during the initial stages of deposition. The departure from linearity noted in Song and Elimelech's model is solely attributable to charge heterogeneity, since a linear Langmuirian blocking function was used in the model rather than a nonlinear blocking function.

For certain idealized collector geometries including spheres, cylinders, and parallel plate channels, the accessibility of the collector surface to particle deposition will vary according to the position on the collector surface. Such collectors are said to have nonuniformly accessible surfaces.[62] The variations in accessibility of the surface to particle deposition produce highly localized surface coverage rates and a correspondingly nonlinear dependence of deposition rate on fractional surface coverage. Song and Elimelech[50,91] modeled nonuniform, localized particle flux onto the surface of spherical collectors. The effects of nonuniform accessibility were then incorporated into a dynamic particle deposition model by means of a

(90) Song, L.; Johnson, P. R.; Elimelech, M. *Environ. Sci. Technol.* **1994**, *28*, 1164.
(91) Elimelech, M.; Song, L. *Sep. Technol.* **1992**, *2*, 2.

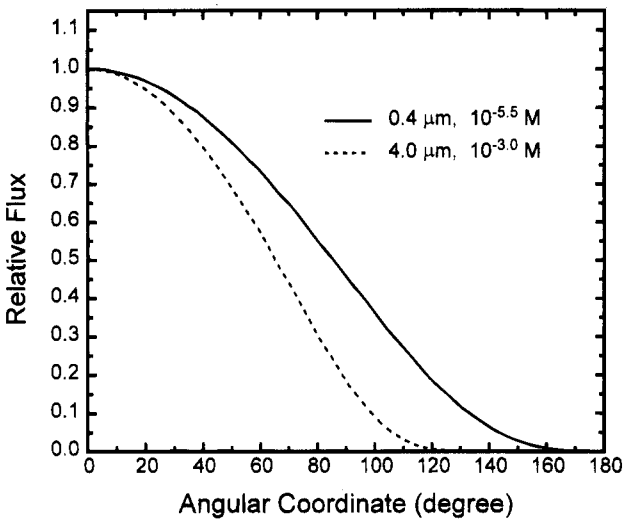

Figure 8. Relative particle flux onto a spherical collector (normalized with respect to the forward stagnation point) as a function of collector angular coordinate. The particle diameter and ionic strength used in the theoretical calculation of each curve are included. The following other parameters were used: surface potential of particles = 40 mV, surface potential of collectors = −20 mV, collector diameter = 0.4 mm, approach velocity = 10^{-3} m/s, porosity = 0.36, Hamaker constant = 10^{-20} J, and temperature = 25 °C.

flux-correcting function.[50] The flux-correcting function is somewhat analogous to a dynamic blocking function in the sense that both characterize the dynamics of particle deposition as a function of surface coverage.

The nonuniform accessibility of a spherical collector as a function of the angular position on the surface is illustrated in Figure 8. The normalized particle flux for Brownian (0.4 μm diameter) and non-Brownian (4 μm diameter) particles is plotted as a function of the angular coordinate on the collector surface with respect to the forward stagnation point at 0°. Figure 8 indicates that the surface of a sphere presents a high degree of variability in terms of its accessibility to particles. As expected, the forward stagnation point (0°) is the most accessible region on a spherical collector, whereas the rear stagnation point (180°) is totally inaccessible to particle flux. The surface accessibility also depends on particle size, with smaller, Brownian particles having greater access to the entire collector surface, especially the lower hemisphere corresponding to the rear stagnation point. The enhanced accessibility of spherical collector surfaces to Brownian particles is a direct outcome of the convective diffusion transport mechanism[50,91,92] whereby submicron-sized particles are transported to a spherical collector surface via convection and Brownian diffusion. On the other hand, larger, non-Brownian particles are largely restricted to the upper hemisphere because of the so-called interception effect.[2,92]

Figure 9 displays the corresponding flux-correcting functions generated from the nonuniformly accessible surfaces described in Figure 8. In addition, a flux-correcting function for a uniformly accessible surface is provided for comparison. The nonuniformly accessible surfaces are shown to exhibit the same characteristic nonlinearity as the RSA dynamic blocking function (Figure 4). Particle size is demonstrated to have an important effect on the departure of the flux-correcting function from nonlinearity. The flux-correcting function for non-Brownian particles exhibits a greater deviation from

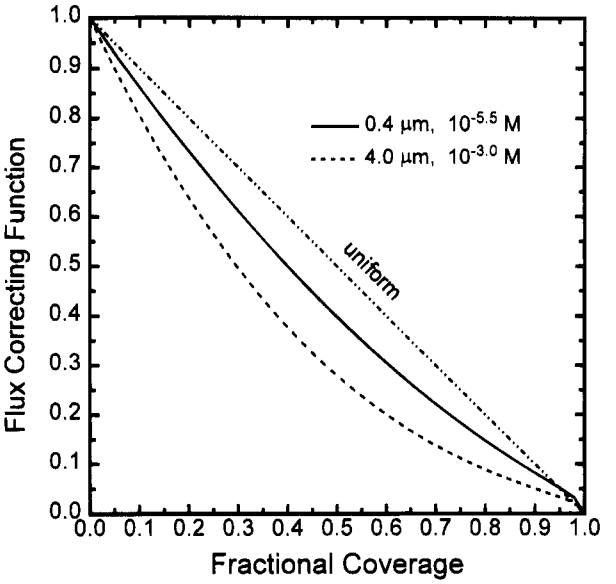

Figure 9. Flux-correcting functions corresponding to the particle flux curves shown in Figure 8. The straight broken line is for uniform deposition, *i.e.*, when the average particle deposition rate is used to represent the deposition onto the entire spherical collector.

nonlinearity than that of Brownian particles because of the higher degree of nonuniformity in surface coverage associated with non-Brownian particles.

It is important to point out that the flux-correcting function for Brownian particles exhibits a nonlinear dependence on fractional surface coverage only at very low ionic strength.[50] As ionic strength increases, the nonuniformity of the localized deposition of Brownian particles diminishes so that the overall effect, when averaged over the entire collector surface, is not pronounced. The same cannot be said for non-Brownian particles, where the flux-correcting function remains highly nonlinear, even at higher ionic strengths (*e.g.* 10^{-3} M in Figure 9). The enhanced nonlinearity associated with non-Brownian particles is attributable to the interception effect, which causes a high degree of nonuniformity in particle deposition.

We wish to stress that the modeling carried out by Song and Elimelech for surface charge heterogeneity[51] and nonuniform particle deposition[50] was based on a Langmuirian dynamic blocking function rather than a nonlinear blocking function. As a consequence, the nonlinear dependence of deposition rate on fractional surface coverage noted for both surface heterogeneity and nonuniformly accessible surfaces cannot be attributed to surface exclusion effects as characterized by the RSA dynamic blocking function. Future work should focus on combining surface exclusion effects with nonuniform, localized particle deposition to investigate their combined effect on particle deposition dynamics.

4. Conclusion

A particle deposition model is presented that pertains to irreversible deposition of stable colloids in granular porous media. The model contains a dynamic blocking function which characterizes the transient or dynamic aspects of particle deposition attributable to surface exclusion effects. Separate dynamic blocking functions are considered in the model: (i) a nonlinear blocking function derived from random sequential adsorption (RSA) mechanics and (ii) a linear, Langmuirian blocking function commonly found in previous dynamic deposition models. The RSA dynamic blocking function is shown to provide

(92) Yao, K. M.; Habibian, M. T.; O'Melia, C. R. *Environ. Sci. Technol.* **1971**, *5*, 1105.

a more accurate representation of surface exclusion effects because of its nonlinear, power law dependence on fractional surface coverage. Separate theoretical breakthrough curves generated by the model using Langmuirian and RSA dynamic blocking functions are compared to experimental particle breakthrough curves obtained from packed columns of granular material over a wide range of ionic strengths. Results reveal that, for all instances involving irreversible monolayer deposition of stable colloids, the RSA-based deposition model provides a superior fit to the experimental data.

The excluded area exerted by an irreversibly deposited stable particle on a spherical collector surface is shown to be a function of solution ionic strength, as predicted by DLVO theory. The highest values for the excluded area parameter are attained at low ionic strengths when electrical double layers are expanded and particles are "soft". An increase in ionic strength results in reduced values of the excluded area parameter due to compression of the diffuse double layer and "hardening" of particles. The hard sphere jamming limit associated with a spherical collector geometry exhibits local variations on the collector surface because of its dependence on the angular coordinate of a deposited particle with respect to the stagnation points. This localized dependence is attributable to hydrodynamic scattering effects originating from the coupling of fluid shear and electrostatic interactions. A unique, surface-averaged hard sphere jamming limit is associated with a specific set of physicochemical and hydrodynamic conditions for particle deposition onto spherical collectors. Because of hydrodynamic scattering, this unique value will always be less than 0.546, the value determined for stagnation point flow and flat surfaces.

The timing of particle breakthrough and shape of particle breakthrough curves are strongly influenced by solution conditions and travel distance within a porous medium. Solution ionic strength influences the timing of initial breakthrough by controlling the excluded area exerted by particles. An increase in ionic strength results in a delayed initial breakthrough of particles, as a reduction in excluded area allows a greater density of particles to accumulate on collector surfaces. Particle breakthrough curves for long columns are characteristically sigmoidal, having a shape that resembles solute dispersion in a porous medium. However, the sigmoidal shape of the theoretical breakthrough curves is shown to be a product of the irreversible deposition process and surface exclusion effects rather than particle dispersion, since the effects of dispersion are not included in the theoretical model.

Glossary

a_c	collector radius
a_p	particle radius
$B(\theta)$	dynamic blocking function
D_h	hydrodynamic dispersion coefficient
f	specific surface area of collectors
I	solution ionic strength
k	jamming limit slope
K	particle transfer coefficient
L	length of packed column
n	particle number concentration
n_0	influent (inlet) particle concentration
r_0	average pore radius
t	time
t_d	porous medium deposition time
U	approach (superficial) velocity of fluid
v_p	interstitial particle velocity
x	transformed spatial coordinate defined by eq 17a
z	spatial coordinate in vertical direction

Greek Symbols

α	attachment efficiency
β	excluded area parameter defined by eq 15
ϵ	porosity of porous medium
η	single collector efficiency
θ	fractional surface coverage
θ_{max}	jamming limit
θ_∞	hard sphere jamming limit
τ	transformed time coordinate defined by eq 17b
ζ_c	zeta potential of collectors
ζ_p	zeta potential of particles

Abbreviations

DLVO	Derjaguin–Landau–Verwey–Overbeek
RSA	random sequential adsorption
ccp	cubic close-packed
hcp	hexagonal close-packed

Acknowledgment. The authors acknowledge the support of the National Science Foundation under Research Grant BCS-9308118.

LA940916H